Bull Volcanol (2006) 69: 105–108
DOI 10.1007/s00445-006-0062-9

SHORT SCIENTIFIC COMMUNICATION

Mike R. James · Stuart Robson · Harry Pinkerton · Matthew Ball

Oblique photogrammetry with visible and thermal images of active lava flows

Received: 11 January 2006 / Accepted: 8 February 2006 / Published online: 30 May 2006

Abstract Digital images from hand-held cameras are increasingly being acquired for scientific purposes, particularly where non-contact measurement is required. However, they frequently consist of oblique views with significant camera-to-object depth variations and occlusions that complicate quantitative analyses. Here, we report the use of oblique photogrammetric techniques to determine ground-based thermal camera orientations (position and pointing direction), and to generate scene information for lava flows at Mount Etna, Sicily. Multiple images from a consumer grade digital SLR camera are used to construct a topographic model and reference associated ground-based thermal imagery. We present data collected during the 2004–2005 eruption and use the derived surface model to apply viewing distance corrections (to account for atmospheric attenuation) to the thermal images on a pixel-by-pixel basis. For viewing distances of ~100 to 400 m, the corrections result in systematic changes in emissive power of up to ±3% with respect to values calculated assuming a uniform average viewing distance across an image.

Keywords Close-range photogrammetry · Etna volcano · Lava flows · Thermal imaging

Introduction

In order to improve our understanding of how lavas flow and eventually stop, improved measurements of flow evolution and cooling are required (Hidaka et al. 2005). Satellite data are regularly used for monitoring active volcanoes, but the spatial resolutions available for obtaining appropriate temperature information are currently ~30 m in the mid- or near-infrared region (Landsat TM and ASTER data) or greater in the thermal infrared region (60 m for Landsat ETM+ and 90 m for ASTER; Donegan and Flynn 2004; Pieri and Abrams 2004). These dimensions are considerably larger than the spatial variability in thermal structure of lava flow surfaces and thus limit the use of satellite data for constraining cooling models. The recent availability of hand-held thermal imagers offers a potential solution by enabling viewing over distances of order 10^0–10^3 m, increasing spatial resolutions by up to a factor of 10^5 (to ~1 mm). Thus, images acquired by hand-held instruments have the potential to provide a wealth of information for flow models and also provide 'ground-truth' information for the interpretation of satellite data (e.g. Calvari et al. 2005). However, the critical disadvantages which exist in most close-range datasets (strongly oblique viewing angles, unknown imaging geometry and sensor positioning) usually prevent georeferencing and currently constrain quantitative analysis.

The application of digital photogrammetry techniques within volcanology has been generally confined to producing digital elevation models (DEMs) from conventional aerial imagery (Baldi et al. 2000; Kerle 2002) or, more recently, from satellite data (Stevens et al. 2004). On a smaller scale, close-range and oblique photogrammetry has been successfully used for geomorphological research (e.g. Chandler and Brunsden 1995; Lane et al. 2001) and a computer-vision based approach has been recently developed for determining volcano topography from sequences of oblique images (Cecchi et al. 2003).

Here, we show how close-range digital photogrammetric techniques can be used to combine image data acquired from arbitrarily positioned thermal and visible cameras in order to overcome some of the data processing problems inherent in using oblique viewpoints and comparatively low resolution thermal sensors. Automatic photogrammetric and image matching techniques (Papadaki 2002) are

Editorial responsibility A. Harris

M. R. James (✉) · H. Pinkerton · M. Ball
Department of Environmental Science, Lancaster University,
Lancaster, LA1 4YQ, UK
e-mail: m.james@lancs.ac.uk
Tel.: +44-0-1524593571
Fax: +44-0-1524593985

S. Robson
Department of Geomatic Engineering,
University College London,
London, WC1E 6BT, UK

employed to obtain topographic data, and to rectify and georeference visible and thermal images. Determination of the observed surface and camera orientations allows the relevant atmospheric attenuation factor to be calculated for each pixel of the thermal images. We illustrate the application of these techniques using ground-based images of active lava channels and flow fronts on Etna volcano.

Data acquisition

Mount Etna, in Sicily, Italy, has a recent history of both effusive and moderately explosive activity. After about a year of relative quiescence, on 7 September 2004, a small lava vent opened at ~2,800 m a.s.l., at the base of the SE crater. Within a week, two lower vents at the head of the Valle del Bove (at 2,650 and 2,250 m, Fig. 1) had also formed, from which lava flowed east into the valley. Fed at relatively modest effusion rates (~3 m^3 s^{-1}; Burton et al. 2005), the channel-fed flows were cooling limited (Guest et al. 1987) and (during the period of fieldwork) were <2.5 km long, with active flow fronts at the break in slope on the valley floor, south of Monte Centenari (Fig. 2a). Whilst a considerable portion of the flow field developed on steep topography exposed to rock fall hazard, the flow fronts were relatively accessible. Hence, ground based images could be acquired of the flow front and distal channel regions and the data used in this paper were collected on 27 September 2004.

Visible images were acquired with a Canon EOS 300D (3072×2048 effective pixels) fitted with a fixed-focus 28 mm lens, the imaging geometry of which had been pre-calibrated in a laboratory (Robson et al. 1999). Thermal images were obtained with a FLIR ThermaCAM S40 which provides a horizontal field of view of 24° (similar to that of a 50-mm lens on a digital SLR with an APS dimensioned sensor). The sensor is a 320×240 uncooled microbolometer focal plane array, with a spectral range of 7.5–13 μm. The imaging geometry of the thermal camera is non-trivial to calibrate, since targets with a thermal signature are required. Hence, although preliminary calibration has been carried out to refine the imaging geometry model (corrections are dominated by the first order radial distortion term), variations due to required on site focusing adjustments have not yet been fully accounted for.

The photogrammetric technique used on Etna requires a minimum of four known three-dimensional target positions to be observable within each image in order to reliably estimate the camera orientation. Artificial control targets constructed from metal foil were deployed in the field; some large (~50 cm) flat targets were augmented by smaller (~5 cm) 'ball' targets to improve precision at short viewing distances. Target positions were coordinated using GPS (ProMark X) augmented, for relatively close targets, with target-to-target slope distances made using a tape measure. These measurements were included as observations in the photogrammetric network adjustment along with the GPS data.

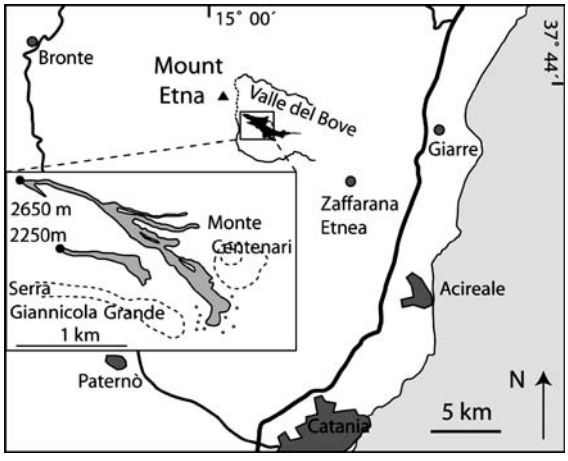

Fig. 1 Geographical location of Etna volcano and the Valle del Bove. The final extent of the 2004–2005 lavas is shown in *black* on the main map and their extent on 27 September 2004 is shown in the *inset* sketch. The *asterisks* surrounding the flow fronts demonstrate the positions of some of the photogrammetric control targets used

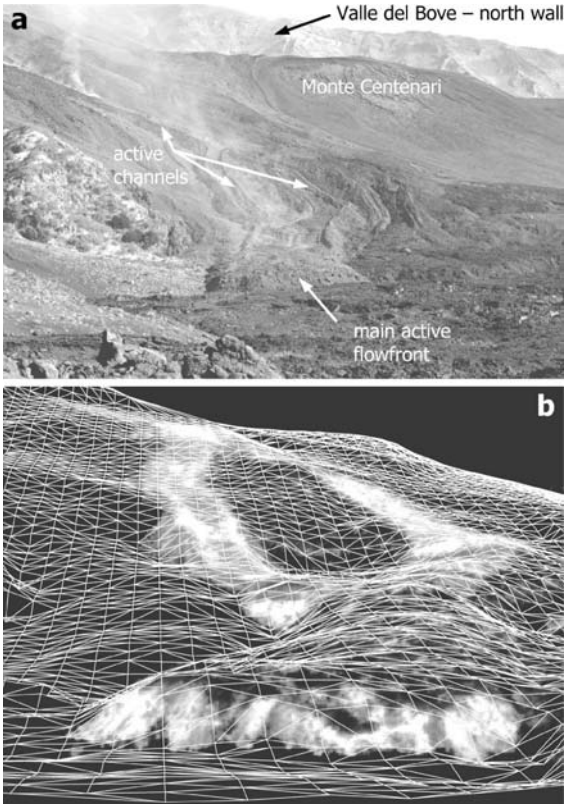

Fig. 2 Visible (**a**) and thermal (**b**) images of the active flow front and channels on 27 September 2004, looking approximately north. For scale, the active flow front is ~35 m wide. The *visible image* shows an inactive flow front and partially drained channel (which had been active during the previous day) to the right of the active front. The *thermal image* is overlain with a perspective view of the triangulated surface model derived from the visible images

Photogrammetry and results

The photogrammetric software employed (VMS, Robson and Shortis, http://www.geomsoft.com) provides a general case geometric solution, suitable for application to networks of convergent oblique imagery. Measurements of each identifiable control target image are used along with the three-dimensional target coordinate data, to provide camera orientation starting values for each image. These initial values are then refined by least squares based resection. If required (e.g. to generate topographic data), additional homologous points can be generated in order to increase the density of the measurement network, before a network or bundle adjustment (Granshaw 1980) is carried out. Registration of the thermal images can be achieved either by using this target-based photogrammetric approach with thermally identifiable targets, or, where a camera position can be ascertained from a visible image taken at the same location, by calculation of relative camera rotation angles only.

Post-processing of the photogrammetric data was carried out using Matlab. A relatively coarse DEM was obtained by interpolating a 4-m triangulated mesh between the topographic data points acquired. Under a suitable projective transformation, the surface can be overlain onto the thermal imagery (Fig. 2b). Obscuration of any part of the surface is handled by depth-ordering the triangulation and considering the closest triangle 'viewed' by each pixel to be the one observed.

In Fig. 2b, temperature data collected with the camera set to a scale of 0–500°C are shown. Viewing distances for the scene vary from ~50 to 400 m and the flow front was ~110 m from the camera. For quantitative analysis of the thermal data, the effects of atmospheric attenuation due to absorption by water vapour should be accounted for. The magnitude of the attenuation for each individual pixel is thus a function of both the relative humidity and the appropriate atmospheric path length. The 'per-pixel' viewing distances required are calculated from ray intersections with the observed topographic triangles. Although external atmospheric correction routines (Berk et al. 1989) could be used, here per-pixel corrections were implemented via similar code within FLIR's ThermaCAM Researcher analysis software. In order to avoid complexities due to mixed-pixel effects (Rothery et al. 1988), temperature values are converted to emissive power (the exitance, W m^{-2}, for radiation of wavelengths between 7.5 and 13 μm) before subsequent analysis. The magnitude of the per-pixel corrections can be observed by comparison with those calculated using an 'average' distance of 200 m across the entire image. Differences between the calculated power values are up to ±3% (increased exitance for distant objects and decreased exitance for closer objects) with respect to the 'globally' corrected image (for a measured relative humidity of 75%).

The combination of a known surface, camera orientation and sensor imaging geometry allows orthorectification of the thermal images and hence georeferencing of the data. An example is shown in Fig. 3. Note that, for this image, some important regions of the flow are occluded by the irregular topography of flow areas closer to the camera. This could be avoided by using less oblique images (e.g. data acquired from a helicopter) or by combining images from different terrestrial positions. Some distortion is evident in the uppermost area of the imaged channel (to the north), where rectification errors from problems at the edge of the surface model are compounded by the oblique viewing angle.

Although these issues will be addressed in future work, flow features can be easily identified in the current rectified data. For example, using the parallel lineations of elevated exitance to delineate the active regions of the channel (as opposed to the levees), at a viewing range of ~310 m, the western channel branch has a width of 17.5 m, which narrows to ~9 m as the flow passes over a region of steeper gradient at a range of ~260 m (Fig. 3). This compares with an average channel width of 17 m and maxima and minima of 37 and 2 m respectively, determined from laser altimeter data collected earlier in the eruption (Mazzarini et al. 2005). For this channel section, the exitance measured from the central region of the flow is ~700–1,700 W m^{-2} (corresponding to a black body temperature of 200–290°C) and up to 4,850 W m^{-2} at the flow margins (corresponding to a black body temperature of ~575°C). The 0–500°C temperature range (used for this image) of the ThermaCam S40 gives saturated values for apparent temperatures >580°C. In this image, 39 pixels were saturated and, with the exception of only a few, these were observing the flow front nearest the camera. However, they represent <0.3% of the imaged front and similar images, taken using the 500–1,500°C temperature range show that the hottest apparent

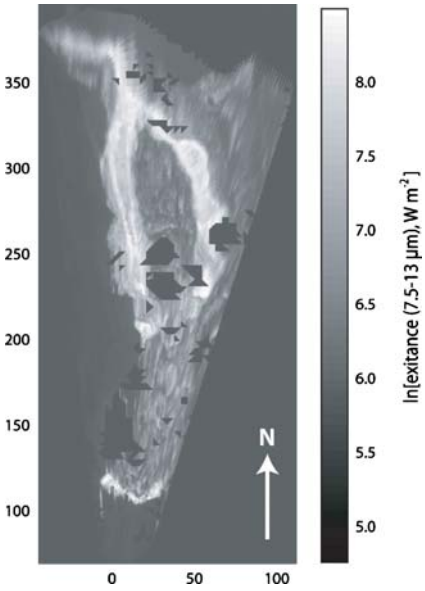

Fig. 3 Orthorectified thermal image. Each pixel value has been corrected for atmospheric attenuation over the relevant viewing distance (ambient temperature, 9.1°C and relative humidity, 75%). *Axes scales* are metres with respect to the camera position. Areas of surface which are occluded for this camera orientation plot in *black*. Their angular nature is a result of defining their extent using the triangulation of the surface model

temperatures in this field of view were ~700°C. The region directly behind the flow front, (at viewing distances of ~110 to 200 m, Fig. 3) displays low exitance values with an average of ~350 W m^{-2} (or ~80°C). In this area, viewing angle is strongly oblique and this non-channelized region of the flow is decelerating over shallow slopes and not exposing hot core material.

The data presented here demonstrate the potential of close-range photogrammetric techniques for imaging lava flows. The thermal image shown (Figs. 2b, 3) illustrates that, in order to maximise the imaged flow area, at least one view with a significantly up- or down-flow orientation should be acquired. Such viewpoints necessitate a per-pixel-based viewing distance correction to account for atmospheric absorption effects which would otherwise result in a systematic error in estimated cooling trends. Knowledge of relative camera orientations (with respect to the imaged surface) is also important for examining the effects of observation angle and resolution on apparent temperature data. Furthermore, registration of this type of imagery, which can be collected at a relatively high repeat frequency, would provide image sequences suitable for quantitive comparisons of flow channel activity and evolution, effusion rate estimates and flow field advance, representing a valuable resource for integration with other datasets and for hazard mapping.

Summary

1. Multi-photo close-range photogrammetric techniques have been successfully applied to visible and thermal images of lava flows collected using ground-based cameras.
2. The visible images have been used to generate topographic data and to assist registration of the thermal imagery.
3. The combination of known imaging geometry and topographic data allows observation distances to be calculated and hence relevant atmospheric attenuation corrections to be applied to each pixel in the thermal images.
4. Photogrammetric orthorectification and georeferencing of the thermal images provides quantitative results for further analysis of lava-flow development (e.g. channel migration, transition from channel to tube morphology, the effect of flow fronts constraining advance rates) and for combination with other image datasets.

Acknowledgements This work was supported by the Royal Society. We thank S. Calvari, J. Dehn, D. Rothery and an anonymous reviewer for thorough reviews which have improved the text.

References

Baldi P, Bonvalot S, Briole P, Marsella M (2000) Digital photogrammetry and kinematic GPS applied to the monitoring of Vulcano Island, Aeolian Arc, Italy. Geophys J Int 142:801–811

Berk A, Bernstein LS, Robertson DC (1989) MODTRAN: a moderate resolution model for LOWTRAN 7. Hanscom Air Force Base, MA: Air Force Geophysics Laboratory, Bedford, MA, p 38

Burton MR, Neri M, Andronico D, Branca S, Caltabiano T, Calvari S, Corsaro RA, Del Carlo P, Lanzafame G, Lodato L, Miraglia L, Salerno G, Spampinato L (2005) Etna 2004–2005: an archetype for geodynamically-controlled effusive eruptions. Geophys Res Lett 32:L09303. DOI 10.1029/2005GL022527

Calvari S, Spampinato L, Lodato L, Harris AJL, Patrick MR, Dehn J, Bruton MR, Andronico D (2005) Chronology and complex volcanic processes during the 2002–2003 flank eruption at Stromboli volcano (Italy) reconstructed from direct observations and surveys with a handheld thermal camera. J Geophys Res 110:B02201. DOI 10.1029/2004JB003129

Cecchi E, van Wyk de Vries B, Lavest JM, Harris A, Davies M (2003) N-view reconstruction: a new method for morphological modelling and deformation measurement in volcanology. J Volcanol Geotherm Res 123:181–201

Chandler JH, Brunsden D (1995) Steady-state behavior of the Black-Ven mudslide: the application of archival analytical photogrammetry to studies of landform change. Earth Surf Process Landf 20:255–275

Donegan SJ, Flynn LP (2004) Comparison of the response of the landsat 7 enhanced thematic mapper plus and the earth observing-1 advanced land imager over active lava flows. J Volcanol Geotherm Res 135:105–126. DOI 10.1016/j.jvolgeores.2003.12.010

Granshaw SI (1980) Bundle adjustment methods in engineering photogrammetry. Photogramm Rec 10:181–207

Guest JE, Kilburn CRJ, Pinkerton H, Duncan AM (1987) The evolution of lava flow-fields: observations of the 1981 and 1983 eruptions of Mount Etna, Sicily. Bull Volcanol 49:527–540

Hidaka M, Goto A, Umino S, Fujita E (2005) VTFS project: development of the lava flow simulation code LavaSIM with a model for three-dimensional convection, spreading and solidification. Geochem Geophys Geosys 6:Q07008. DOI 10.1029/2004GC000869

Kerle N (2002) Volume estimation of the 1998 flank collapse at Casita volcano, Nicaragua: a comparison of photogrammetric and conventional techniques. Earth Surf Process Landf 27:759–772

Lane SN, Chandler JH, Porfiri K (2001) Monitoring river channel and flume surfaces with digital photogrammetry. J Hydraul Eng 127:871–877

Mazzarini F, Pareschi MT, Favalli M, Isola I, Tarquini S, Boschi E (2005) Morphology of basaltic lava channels during the Mt. Etna September 2004 eruption from airborne laser altimeter data. Geophys Res Lett 32:L04305. DOI 10.1029/2004GL021815

Papadaki H (2002) Accuracy of dense surface measurements in an integrated photogrammetry and machine vision framework. Int Arch Photogram Remote Sensing 34:68–73

Pieri D, Abrams M (2004) ASTER watches the world's volcanoes: a new paradigm for volcanological observations from orbit. J Volcanol Geotherm Res 135:13–28

Robson S, Shortis MR, Ray SF (1999) Vision metrology with super wide angle and fisheye optics. In: Videometrics VI. SPIE Volume 3641, SPIE, San Jose, pp 199–206

Rothery DA, Francis PW, Wood CA (1988) Volcano monitoring using short wavelength infrared data from satellites. J Geophys Res 93:7993–8008

Stevens NF, Garbeil H, Mouginis-Mark PJ (2004) NASA EOS Terra ASTER: volcanic topographic mapping and capability. Remote Sens Environ 90:405–414